**Sixth International Conference on Durability of Concrete Structures** **Paper Number TIM16**
**18 - 20 July 2018**
**University of Leeds, Leeds, West Yorkshire, LS2 9JT, United Kingdom**

# Damage Evaluation of Full-Scale RC Slab by Ultrasonic Tomography

H. Hayashida
Materials Research Team, Cold-Region Maintenance Engineering Research Group, Civil Engineering Research Institute for Cold Region, Sapporo JAPAN

T. Ueda
Division of Engineering and Policy for Sustainable Environment, Graduate School of Hokkaido University, Sapporo, JAPAN

## ABSTRACT

*There have been reports of road bridges that deteriorated after their RC slabs had been repaired. The insufficient removal of damaged materials is thought to be the cause of such post-repair deterioration. Consequently, a survey method that is able to detect deteriorated materials in slabs with high accuracy has been called for. Toward the development of such a method, this report focuses on ultrasonic tomography, because it is able to detect damage to the RC slabs of road bridges over relatively large areas. We examined the applicability of ultrasonic tomography to a method for assessing the RC slab damage by a test that uses a full-scale RC slab specimen that had been deteriorated by repeated loading on a wheel-tracking test machine. The results show that ultrasonic tomography excelled at detecting areas of punching shear damage but was not able to clearly detect horizontal cracks that coexist with damage from compressive stress.*

**Keywords:** wheel-tracking test, fatigue, RC slab, ultrasonic tomography, micro cracks

## 1.0 INTRODUCTION

Aging of the road bridge RC slabs constructed during Japan's period of high economic growth has been progressing, and these slabs have undergone repairs and reinforcement. In works such as those for increasing the thickness of the upper surface of the slab or those for the partial replacement of the slab, the deteriorated parts are removed, for example by using a water jet, and repair is done by the placement of patching materials.

However, some cases have been reported of premature re-deterioration to such RC slabs that had been repaired by using the above described techniques (Japan Society of Civil Engineers, 2016). It was clarified that one cause of such re-deterioration was the insufficient removal of the deteriorated parts (Naito *et al*., 2010). An example of procedures for determining the range of deterioration (i.e., the range for removal) in a road bridge RC slab follows. 1) To clarify the planar distribution of damage, tests such as the hammering sound test are done. 2) To clarify the damage distribution in the direction of the slab depth, core sampling locations are determined based on the planar distribution of the damage. 3) The depth of damage is assessed from the cracking of the cores and from regions of decreased ultrasonic velocity. 4) The range for the removal of damaged parts is set based on a comprehensive assessment of the planar distribution of damage, locations of coring, and the depth of damage.

In the above-described procedures, the depth for removal in a certain range is set by setting a representative value regarding the damage depth, which is determined from localized information obtained from coring locations. However, in actual road bridge RC slabs, the degree and location of vehicle passage and water supply differ for various positions on the slab; therefore, it is possible that the actual depths of damage exceed those set in the above-described procedures. Furthermore, it is possible that, in actual repair work, the removal of the deteriorated part is insufficient because such removal is done based on the originally designed values.

To prevent the premature re-deterioration of repaired slabs, it is necessary to establish mechanisms for accurately removing the deteriorated parts during repairs, and it is necessary, in designing RC slabs, to establish a system for accurately determining the severity of any deterioration.

Here, the mechanism behind the progress of damage in road bridge RC slabs is examined, including by microscopic examination. Based on

previous findings (Mihashi, Kunieda and Rokugo, 2010), fatigue failure in concrete that receives repeated loading is thought to occur after the following three processes.

1) Cracking occurs around large aggregate, and the propagation of that cracking is blocked by abutting aggregate.

2) Damage (micro cracks) accumulates at the boundary between the matrix and the aggregates.

3) Localized propagation occurs, and the cracks progress.

The grid-shaped cracks that occur on the underside of a road bridge RC slab and the horizontal cracks, about which some issues have been raised in recent years, are cracks that locally progress and fall in the stage of #3 above. When the mechanism described above is considered, it is thought that there are regions where micro cracks accumulate in areas surrounding the localized cracks. In damage inspection, it is necessary to clarify all damage, including macro and micro cracks.

This report focuses on ultrasonic tomography, a non-destructive inspection technique for detecting damage, including micro cracks, that occurs in comparatively wide areas of road bridge RC specimen slabs. To collect basic data for examining the relationship between the actual damage and the analysis results of the test using ultrasonic tomography, an investigation was done by using a full-scale RC slab that had experienced fatigue in the wheel running test and ultrasonic tomography.

## 2.0 OUTLINE OF THE INVESTIGATION

Ultrasonic tomography in which the ultrasonic velocity is used to determine the condition of the specimen was done for the specimen slab that had undergone fatigue in the wheel running test. The reason for selecting ultrasonic tomography in this investigation is as follows. Ultrasonic wave inspection uses waves with relatively high frequencies; therefore, the wave lengths are short and the accuracy in detecting small internal defects is high. The possibility of accurately detecting micro cracks from fatigue, which were the subject of the experiment of this report, was thought to be high.

To verify the effectiveness of ultrasonic tomography, its results were compared to those obtained by ultrasonic propagation velocity measurement of cores (transmission method) and investigation of cracks by injecting fluorescent epoxy resin, which have been used in actual damage inspections for the road bridge RC slabs. The comparison investigation is outlined in the following sections.

### 2.1 Specimen Slab

The shape and dimensions of the specimen slab and the reinforcing bar arrangement are shown in Fig. 1. The specimen was 3000 mm × 2000 mm, was 160 mm in thickness, and was designed based on the Specifications for Highway Bridges (1964). The authors planned to use the specimen slab for investigations on combined deterioration from fatigue and frost damage by conducting freeze-thaw tests after the wheel running test; therefore, no air-entraining agent was used and the water to cement ratio was set at 68 %, which is rather high, because it was necessary to promote frost damage at an early stage. The compressive strength at 4 weeks of standard curing was 24.5 N/mm$^2$. Ordinary Portland cement and crushed stone with a maximum coarse aggregate size of 20 mm were used.

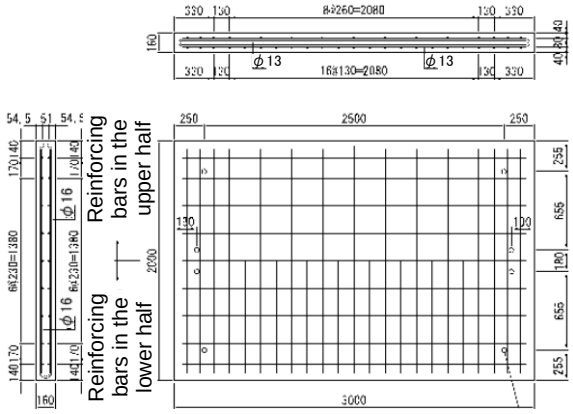


**Fig. 1.** The shape and dimensions of the specimen slab and the reinforcing bar arrangement

### 2.2 Wheel Running Test Machine

After 4 weeks of moist curing, the wheel running test was conducted.

<u>The Wheel Running Test Machine, and the Supporting Conditions</u>

The wheel running test machine used in this experiment was of the crank type (the iron wheel type, Fig. 2). The fly wheel is rotated by the motor and the rotational motion of fly wheel is converted to the reciprocating motion of the iron wheel via the crank rod. Two conditions for supporting the edges of the specimen were used: simple support on the two long sides (in the wheel movement direction) and relative elastic support on two sides (in the direction of the span) in which the support considered unidirectional loading on the bridge slab.

<u>Deterioration Target, Running Load, and Number of Runs</u>

The degree of deterioration of the specimen slab set as the target was the deterioration at the design bending value of 3.0 mm, in which the condition of the concrete on the tension side was ignored because the purpose of using the slab specimen was to investigate the ultrasonic tomography;

therefore, the deterioration of the specimen was set as that before the failure of the specimen.

**Fig. 2.** Wheel running test machine

The running load was set at the relatively small value of 110 kN, because in a wheel running test with a relatively great running load such as that used for determining the fatigue life of the specimen, it was feared that bending would suddenly increase during the test and exceed the deterioration target. The running load during the wheel running test was kept constant.

In the wheel running test using this running load, the number of runs before the design bending value was attained was 110,000. Cracks in the slab at the end of the wheel running test are shown in Fig. 2. The cracks on the underside are indicated by thin lines, and the cracks on the top surface are indicated by thick lines.

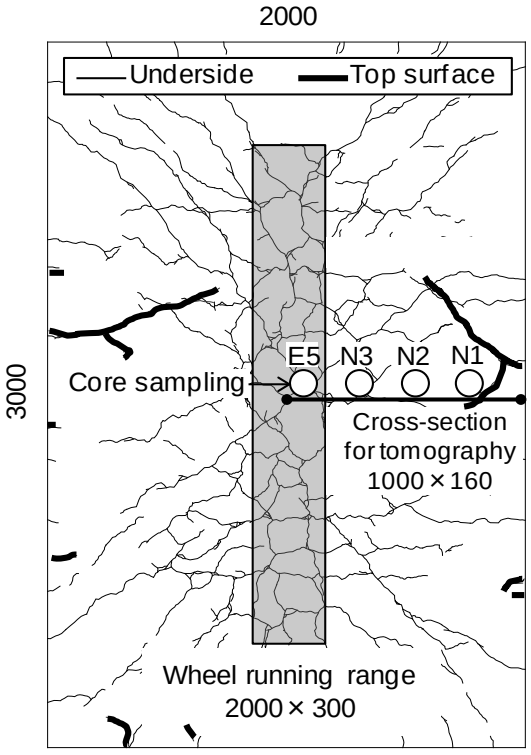


**Fig. 3.** Cracks in the slab after the wheel running test

### 2.3 Ultrasonic Tomography Analysis of the Slab Specimen

Calculation Procedure

The analysis used ultrasonic tomography analytic software developed by Yamashita *et al*. (Yamashita, Sakai, Kumagai and Kita, 2000.) The procedure for the analysis is shown in Fig. 4. First, the range for this investigation on the slab was divided into a finite number of elements in a grid pattern. Each element was supposed to have an individual value of ultrasonic propagation velocity. When the propagation path (a linear wave profile) of an ultrasonic wave for a given wave line *i* is considered, the propagation distance of the wave motion *li* is obtained as the total sum of the line segment length *Δlij* on which the wave line *i* passes through the tomographic element *j*. When the ultrasonic velocity of line segment *Δlij* in a given element *j* is assumed to be *Vj*, the calculated propagation time *Ti* between the oscillation point and receiving point is expressed as Eq. (1).

$$T_i = \sum_{j=1}^{m} \left( \Delta l_{ij} / V_j \right) \quad (1)$$

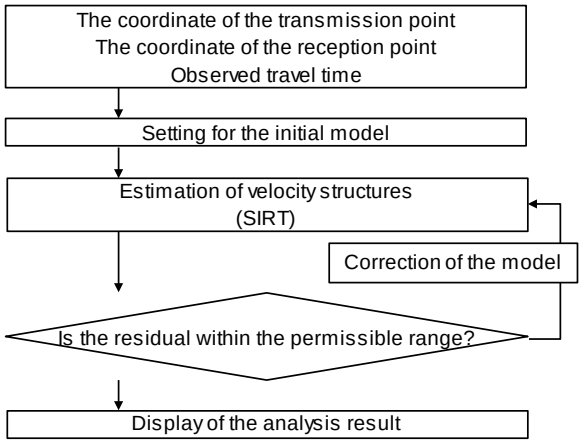


**Fig. 4.** Procedure of the ultrasonic tomography analysis

Next, the propagation time obtained from Eq. (1) and the measured propagation time were compared and the ultrasonic velocity in the element was corrected. This calculation was repeated until the cumulative total of the absolute value of the difference between the measured and the calculated values on each measurement line became the preset standard value or lower. As a method for correcting the errors between theoretical travel-time and observed travel-time, this software uses the SIRT method for correcting the velocity model.

Analysis Cross Section, Region for Analysis, and Division into Elements

For the analysis cross section, which is shown in Fig. 3, a cross section was selected that is

perpendicular to the direction of wheel travel and is at the center of the specimen. (The length in the direction perpendicular to the travel direction (X) was 1000 mm and the length in the thickness direction (Z) was 160 mm.) The reason for selecting a cross section that was at the center of the specimen and in the direction perpendicular to the wheel travel direction was as follows. In a previous study (Nakatani, Uchida, Nishikawa, Kanda, Miyazaki, Kawama and Matsuo, 2002.), cracking from punching shear was found in the cross section with a direction perpendicular to the wheel traveling direction. The cracking from punching shear was thought to be generated from localized cracks that propagated and progressed. It is thought that there are regions around these cracks where micro cracks accumulate from repeated loading. It was thought that the selected cross section was appropriate for investigating a method of detecting micro cracks by ultrasonic tomography, because the selected cross section in the direction perpendicular to the wheel travel direction included a region with accumulated micro cracks.

As shown in the top half of Fig. 5, the region for this analysis, which was 1000 mm in width, was divided into five segments. Each segment was 200 mm in width and 160 mm in height. As shown in the bottom half of Fig. 5, the propagation time for ultrasonic waves was measured in each divided region, in which sources and receivers were set on the top surface and underside of the specimen. The measurements were taken when the bending of the specimen reached the design bending value, which was measured by ignoring the conditions of the tension side concrete, and the wheel running test was stopped. The sensor used for this measurement was the same sensor as that used for measuring the ultrasonic propagation velocity of the sampled cores, which will be discussed later in this report. The reason for dividing the analysis cross section into 5 segments was that even though the ultrasonic waves can detect small internal damage with high accuracy because they have a relatively high frequency, the attenuation of the wave in concrete is great and the propagation distance becomes short in damaged concrete.

Then, as shown in the bottom diagram in Fig. 5, the calculation was done by dividing the area of 200 mm by 160 mm into 20 elements: the width of each 200 mm-segment was divided into 5 and the height of 160 mm was divided into 4. In the expressing the analysis result, smoothing processing was done by subdividing each element into 9.

### 2.4 Ultrasonic Propagation Velocity of the Cores (Transmission Method)

Four cores were collected at the locations shown in Fig. 3. In a way similar to that used in actual inspections for determining the depth of damage in road bridge RC slabs, the ultrasonic propagation velocity (hereinafter, the ultrasonic velocity) was measured by setting measurement lines at intervals of 20 mm in the direction of the height of the specimen as shown in Fig. 6. The measurement lines for the ultrasonic velocity were set such that the lines would be parallel to the cross-section for tomographic analysis. In the investigation for this report, an ultrasonic wave device (Fig. 6) was selected that is used in actual inspections for concrete structures and is relatively easily available. This device measures the propagation time of ultrasonic waves from transmission to reception with a resolution of 0.1 μs. The measured values are displayed on the digital display of the device. The sensor has a resonance frequency of 28 kHz, a voltage of 1 KV, and a sensor diameter of φ 20 mm.

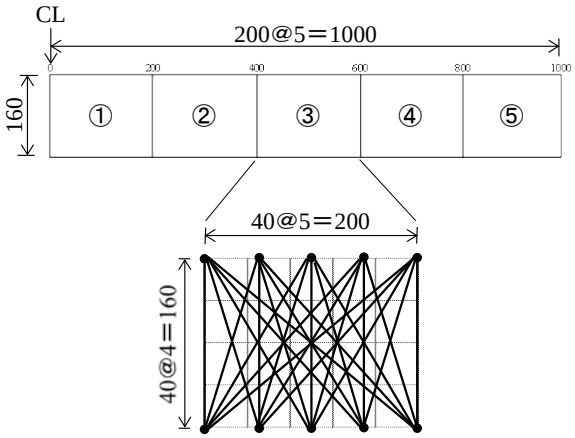


**Fig. 5.** Analysis cross-section, region for analysis, and division into elements

### 2.5 Identification of Cracks by Injection of Fluorescent Epoxy Resin

The cracks in the cores were identified by using a method in which fluorescent epoxy resin was injected. The procedure of the method is explained below.

1) After the ultrasonic velocity was measured, fluorescent epoxy resin was injected in the cores.

2) The cores were cut by concrete cutter such as to reveal the cross-section that was parallel to the cross-section for the tomographic analysis.

3) The condition of cracks was examined by using a microscope to observe the cutting plane.

## 3.0 RESULTS AND DISCUSSION

The results of the ultrasonic tomography analysis are shown in Fig. 7, and the cracks identified by fluorescent epoxy resin injection and the results of ultrasonic velocity measurement are shown in Fig. 8. The ultrasonic velocity ratio (the horizontal axis of

the graph) in Fig. 8 is the ratio of the measured ultrasonic velocity of the cores to the ultrasonic velocity of 1.0 for the height of 1 cm of Core N1, which is thought to be largely sound and whose ultrasonic velocity is the highest among any of the cores. To clarify the relationship between the absolute value of the ultrasonic velocity ratio and the absolute value of the ultrasonic velocity, the ultrasonic velocity ratio of the core is indicated at 0.1 intervals under the legend of the velocity in the ultrasonic tomography shown at the top of Fig. 7. The following explains the investigation result for each core.

### 3.1 Core E5

Conditions of Cracking

Core E5 is from immediately below the loading range, and as shown in Fig. 8 (a), horizontal cracks were found at heights of about 14 – 12 cm.

The Results of Tomographic Analysis

*(a) The area near the horizontal cracks*

In the top of Fig. 7, the ultrasonic velocity calculated for near the horizontal cracks (hereinafter, the velocity) is not constant. The velocity is lower in the left area than in the right area. The reason for the differences in velocity will be discussed in (b).

*(b) Region A*

The velocity for Region A shown in the top figure of Fig. 6 is low relative to the velocities for the regions around it. This region is thought to have received compressive stress and damage because it is near the center of the wheel track and at the upper edge of the specimen. The difference in velocity in the areas near the horizontal cracks is thought to be because damage from compressive stress and damage near the horizontal cracks are mixed in this area. The damage (cracks) from compressive stress are not identified in the Fig. that shows the cracks in the core. It is possible that micro cracks, which are not identifiable by fluorescent epoxy resin injection, occurred. In the other cores, which will be discussed later, the ultrasonic velocity was low; however, micro cracks were not found in the fluorescent epoxy resin injection. Possible reasons for the above are given here; however, the details will be examined in the future studies.

1) In the compression range of concrete that receives repeated loading, a phenomenon similar to the strain hardening of metal material (Kishitani, Nishizawa, *et al*., 1987) occurs and micro cracks close.
2) During the wheel running test, the micro cracks open and close repeatedly. At the end of the test, the micro cracks are closed because the load that opened the cracks is not acting on the specimen.
3) Even though the epoxy resin used is of low viscosity, the micro cracks were extremely narrow and the injection pressure was insufficient for sending the epoxy resin into those fine cracks.

*(c) Region B*

The velocity for Region B shown in the top figure in Fig. 6 is low relative to the velocities for the regions around it. The low velocity found in Region B is thought to be related to the flexural cracks generated by the wheel loading. The reason for the above is as follows. As shown in the bottom figure in Fig. 6, flexural cracks are found in the part of Region B on the bottom surface of the specimen. A previous study (Mihashi *et al.*, 2010) pointed out that micro cracks that were too small to be seen by the naked eye accumulated around the cracks that were generated by tensile stress. In the current study, it is though that the velocity in Region B was low because of the flexural cracks generated by wheel loading and micro cracks at and around the flexural cracks.

Ultrasonic Propagation Velocity of the Cores (Transmission Method)

As shown in Fig. 8 (a), the ultrasonic velocities at the heights of 15 cm and 13 cm are considerably low. In light of the condition of cracks and the analysis results of tomography, these low velocities are thought to result from damage caused by compressive stress and damage near the horizontal cracks. The degree of lowering in the ultrasonic velocities at the locations from the heights between 11 cm and 1 cm is small; however, the ultrasonic velocities mildly decrease as the waves approach to the lower end of the core. This lowering of ultrasonic velocities is thought to be from the micro cracks discussed in (2) (c).

Comparison between the Velocity of the Core and the Velocity in the Tomographic Analysis

The ultrasonic velocities for the cores tend to be higher than those from the tomographic analysis. For example, the velocity (absolute value) of the core at the height of 11 cm is about 3700 m/s, while the velocities at the height of 11 cm in the tomographic analysis are about 2250 – 1750 m/s. This tendency is seen, with differences to some degree or another, in all the results of ultrasonic velocity measurement. It is possible that there is a reason for the above as follows; however, the details will be examined in the future studies. A previous study (Ishigami *et al.*, 2014) clarified that the ultrasonic velocity increases with the increase in water content. Water was used in the core drilling; therefore, it was possible that the water content of the core at the time of ultrasonic wave measurement was higher than the water content of the slab specimen. It was possible that the ultrasonic velocity became higher than the ultrasonic velocity of the specimen slab, which was determined in the tomographic analysis, because of the influence of this water.

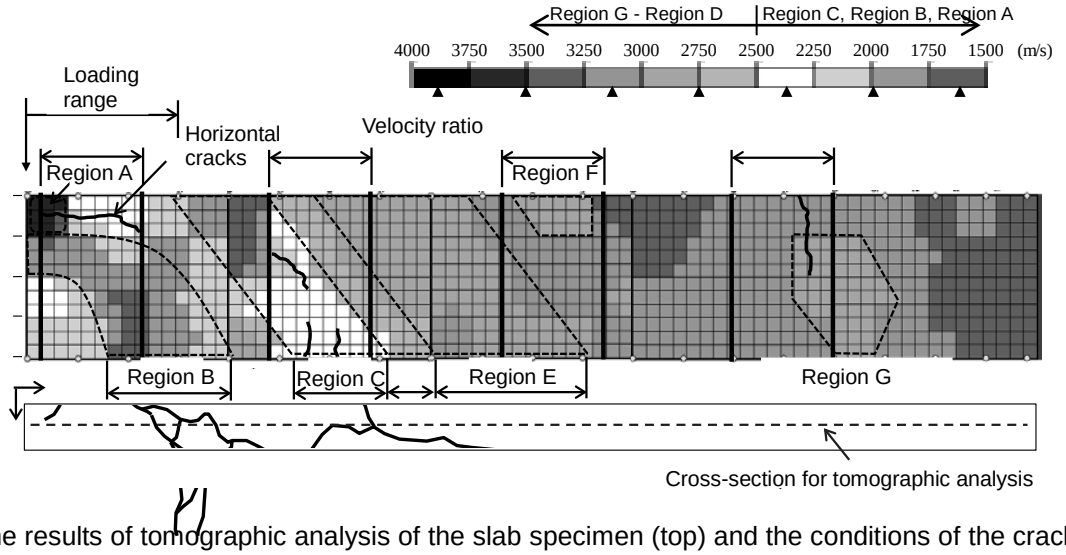


**Fig. 7.** The results of tomographic analysis of the slab specimen (top) and the conditions of the cracks on the underside (bottom)

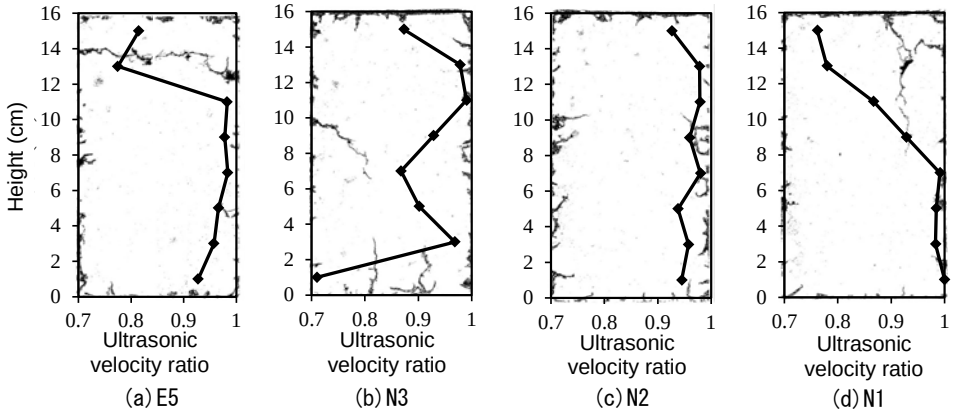


**Fig. 8.** The conditions of cracks on the cross sections of the cores and the results of ultrasonic velocity measurement

### 3.2 Core N3

Conditions of Cracking

Core N3 is from near the edge of the loading range where cracks from punching shear are generally thought to occur. As shown in Fig. 8 (b), the existence of diagonal cracks around the heights of 10 – 7 cm and the occurrence of vertical cracks around the heights of 3 – 0 cm are observed.

The Results of Tomographic Analysis

*(a) Region C*

The results of tomographic analysis for the location of Core N3 shown in the top of Fig. 7 shows that the velocity of Region C is low compared to those in the surrounding regions. Region C extends from the edge of the wheel loading range on the top surface of the specimen slab diagonally downward. The cracks discussed in (1) are in Region C. In light of their location and direction, these cracks are thought to appear after micro cracks had developed, accumulated and reached their limit of being micro cracks by punching shear. Based on the above, ultrasonic tomography is thought to be good for identifying the regions damaged by punching shear.

*(b) Region D and Region E*

Regions D and E, which abut Region C, were found to distribute diagonally and parallel to Region C, which is the region damaged by the punching shear. The velocities in Regions D and E gradually become smaller as one move away from the center of the wheel running track.

Ultrasonic Propagation Velocity of the Cores (Transmission Method)

As shown in Fig. 8 (b), the ultrasonic velocities are very low in areas from the heights of 11 cm to 7 cm and in areas from the heights of 3 cm to 1 cm, both of which are areas with cracks that were discussed in (1). Similar to Core E5, the ultrasonic velocity at the point with a height of 15 cm, which is close to the top edge of the specimen, is much lower than those of other areas.

### 3.3 Core N2

As shown in Fig. 8 (c), marked cracks are not found in Core N2. The results of tomographic analysis for the location of Core N2 in the top figure of Fig. 7, in addition to Region E described earlier, show that the velocity of Region F is lower than those in the surrounding regions. Next, the ultrasonic velocities of cores shown in Fig. 8 (c) are examined. The degree of decrease in the ultrasonic velocity is small as a whole; however, the ultrasonic velocity at the locations from the height of 1 cm to 5 cm is low, which corresponds to the velocity in Region E, and the ultrasonic velocity at the location at the height of 15 cm is low, which corresponds to the velocity in Region F. The low velocity in Region F is thought to be from either punching shear damage or compressive stress damage.

### 3.4 Core N1

As shown in Fig. 8(d), vertical cracks are seen in the area from the top edge down to about the height of 8 cm. These cracks are observable on the upper surface of the specimen slab, as shown by the thick lines in Fig. 3. These cracks are thought to be generated by negative bending, because Core N1 was close to the supporting point in the wheel loading test. Next, as shown in the top figure of Fig. 7, Region G, which is a region with low velocities in the tomographic analysis, exists on the right side of Core N1. The cracks in Region G may have been generated by negative bending, because they are in the direction of progress of the vertical cracks. Next, regarding the ultrasonic velocity of the core shown in Fig. 8(d), the velocity greatly decreased from the point 7 cm in height to the point 15 cm in height, which seems to correspond to the distribution of the vertical cracks. However, no decrease in velocity that corresponds to the distribution of the vertical cracks is seen in the tomographic analysis shown in the top of Fig. 7. The reason for the above is thought to be as follows. During the wheel running test, the micro cracks opened and closed repeatedly. After the end of the test, the micro cracks closed because the load that opened the cracks was no longer acting on the specimen. Because of the closed micro cracks, the velocity did not decrease around the cracks at the measurement of the ultrasonic propagation velocity of the specimen slab. In the cores, which were used in the measurement of ultrasonic velocity and for fluorescent epoxy resin injection, the micro cracks were open because the confining pressure that had been acting on the specimen was released when the core was taken from the specimen slab. Because of these open cracks in the cores, the velocities in the areas surrounding the cracks decreased and the cracks were clearly identified by the injected fluorescent epoxy resin.

## 4.0 CONCLUSIONS

Ultrasonic tomography was done to investigate cracking in a full-sized RC slab specimen that had experienced fatigue. The following are the results of the investigation.

(1) The ultrasonic tomography was well able to detect areas of punching shear damage, but was unable to clearly detect areas of horizontal cracking, whose causes of generation included both punching shear and compressive stress.

(2) The lowering of the ultrasonic velocity in the cores and the results of ultrasonic tomography suggest that, in addition to the macro cracks that occurred in the slab specimen, there was the possibility of micro cracks having occurred.

(3) However, the micro cracks were not identified in the fluorescent epoxy resin injection for the slab, because the injection pressure was not sufficient and the micro cracks were thought to be closed at injection.

**References**

Ishigami, A., Sato, S., Suto, M., Makanae, H., 2014. Water absorption and its effect on the ultrasonic pulse velocity of concrete that has undergone freeze-thaw damage. Cement Science and Concrete Technology, 67:413-420.

Japan Society of Civil Engineers, 2016. Manual for the maintenance of highway bridge decks.

Kishitani, K., Nishizawa, N., *et al*., 1987. Series on the durability of concrete structures: fatigue. Gihodo Shuppan Co., Ltd.

Mihashi, H., Kunieda, M., Rokugo, K., 2010. Cracks in concrete and the mechanics of fracture. Gihodo Shuppan Co., Ltd.

Naito, I., *et al*., 2010. A study on the re-deterioration of surface-coated sluice structures due to frost damage. FraM-CoS7, 1077-1083.

Nakatani, S., Uchida, K., Nishikawa, K., Kanda, M., Miyazaki, K., Kawama, S., Matsuo, S., 2002. Experimental study on the fatigue durability of highway bridge slabs. Technical Note of the National Institute for Land and Infrastructure Management, (28).

Yamashita, H., Sakai, T., Kumagai, M., Kita, T., 2000. Using an ultrasonic method to evaluate concrete quality. Proceedings of the Japan Concrete Institute, 22(1):361-366.